CSCE 2013 General Conference - *Congrès général 2013 de la SCGC*

Montréal, Québec
May 29 to June 1, 2013 / *29 mai au 1 juin 2013*

Buckling Response of Bolted Mid-Connections in Steel X-Bracing

A. Gélinas[1], R. Tremblay[1], and A. Davaran[1]

[1]Group for Research in Structural Engineering Department of Civil, Geological and Mining Engineering, Ecole Polytechnique, Montreal, QC, Canada, H3C 3A7.

Email: robert.tremblay@polymtl.ca

Abstract: A quasi-static cyclic test program was conducted on full scale X-bracing systems of the conventional construction and moderately ductile seismic categories. The study focused on the influence of typical bolted connections at the brace intersection point on the brace stability. HSS bracing members with single and double shear lap splice connections were examined. Braces built with back-to-back double angle sections were also investigated. The test specimens were designed and detailed in accordance with the CSA S16-09 standard. The test program showed that common mid-connections may trigger premature instability of X-braced frame assemblies. In most cases, inelastic response concentrated in the connections, which then became the energy dissipating elements of the system rather than the bracing members. This behaviour generally resulted in limited ductility. Locally increasing the flexural stiffness and strength of the connections could improve the stability response of the system.

1 Introduction

Steel concentrically braced frames (CBFs) in the X configuration are commonly used to resist wind and seismic lateral loads in steel structures. At the intersection of the braces, one bracing member is continuous whereas the other one must be interrupted; a mid-connection detail is therefore needed to transfer loads between the two segments of the discontinuous brace. Square hollow sections (HSS) are often preferred for the bracing members due to their superior compressive resistance per unit weight compared to other sections. In that case, a bolted mid-connection detail is usually achieved by inserting a plate through the continuous brace and connecting the discontinuous braces to that middle plate by means of bolted shear lap joints (Figure 1a). Two configurations can be used: single shear (SS) splice joint or double shear (DS) splice joint. The SS configuration is easier to assemble in the field but has inherent out-of-plane eccentricity. The DS configuration is concentric and is generally shorter because the bolts resist loads in double shear. Braces can also be double angle sections arranged in a back-to-back configuration. In that case, the mid-connection is simpler as the discontinuous brace segments can be directly bolted to the middle plate passing through the two angles forming the continuous brace.

For seismic applications, concentrically braced frames are expected to dissipate seismic input energy through brace yielding in tension and inelastic buckling in compression (CSA 2009). Brace buckling imposes rotation and/or moments at the brace end connections and special detailing requirements are prescribed in codes to ensure ductile rotational response for braced frames designed to achieve high energy dissipation capacity. One approach consists in detailing the middle plates with a minimum free hinge distance equal to 2 times the plate thickness to accommodate the anticipated inelastic rotation.

a)  b) 

Figure 1 : a) Typical bolted mid-connection for HSS members; b) Buckling of a mid-connection between double angle bracing members during the 2011 Tōhuku earthquake in Japan (EERI 2011).

The compressive resistance of a bracing member is obtained by using an effective length, KL, where the brace effective length factor K takes into account the end conditions of the brace. Past research has shown that the tension brace in X-bracing can prevent out-of-plane buckling of the compression brace over its full length. Based on tests, Astaneh-Asl et al. (1985) and Picard and Beaulieu (1988) suggested that a K factor of 0.5 can be used when the brace tension and compression forces are equal, i.e., to consider that out-of-plane buckling will develop between the corner gusset plates and the mid-connection. Recent numerical work has demonstrated that the rotational stiffness and detailing of the brace end connections may influence the brace K factor (Segal and al. 1994, Davaran 2001, Davaran and Hoveidae 2009). However, the effect of possible local out-of-plane deformations of mid-connection components on the stability of the compression braces in X-bracing has not been investigated yet. Such a localized instability mode was recently observed after the 2011 Tōhuku Japan earthquake (Figure 1b), suggesting that this limit state should be considered in design. This paper describes the buckling response of typical X-braced frames with HSS and double angle bracing members with bolted connections as obtained from an extensive full-scale cyclic quasi-static test program.

2 Description of the Test Program

The test program was conducted at the Structural Engineering Laboratory at Ecole Polytechnique of Montreal. The bracing members were installed in an 7.5 m wide by 4.087 m high vertical steel frame. A displacement test protocol consisting of stepwise incremented displacement cycles was applied horizontally at the top of the frame by two high performance hydraulic actuators capable of developing a total horizontal force of 2000 kN (Gélinas et al. 2012).

The test program included 17 test specimens that were designed according to the CSA S16-09 design standard (CSA 2009). The behaviour of 14 of these specimens is reported in this paper. The bolted connection details for these specimens are presented in Figure 2 and the characteristics of the specimens are given in Table 1. Specimens nos. 5 to 14 were built with HSS bracing members assembled with typical bolted connections in the single shear (SS) or double shear (DS) configuration. Two HSS member sizes were used. Specimen no. 9 was identical to Specimen no. 7 except that a stiffener was added for the former to increase the connection flexural stiffness and strength (Figure 2b). In Specimen no. 4, the brace connections were designed with angles welded to the HSS and bolted to the middle plates (Figure 2c). Braces in Specimens nos. 16 to 18 were back-to-back angles and a typical connection design is presented in Figure 2d. A top view of the SS and DS splice connections of Figure 2a are presented in Figure 2e and 2f. At the mid-connection of all specimens, a free distance e_i = 25 mm was left between the end of the discontinuous brace and the middle plate for installation purposes. The HSS braces were made of ASTM A500, gr. C square tubing. G40.21-300W and 350W materials were used for the angles and the connecting parts, respectively.

In Table 1, b_g is the width of the middle plate, t_g is thickness of the middle plate, n_b is the number of bolts, d_b is the diameter of the bolts, T_{fc} and C_{fc} are respectively the factored connection design loads in tension

and compression, C_r is the design factored compressive resistance of the brace, $C_{ue,Dis}$ and $C_{ue,Con}$ are the measured compressive resistances of the discontinuous and continuous braces, respectively. It is noted that $t_g = t_s$ for the SS connections whereas $t_g = 2\ t_s$ for the DS connections, where t_s is the thickness of the splice plates. The width of the middle and splice plates were the same ($b_g = b_s$), except for Specimen no. 11 where t_s = 7.9 mm and b_s = 240 mm.

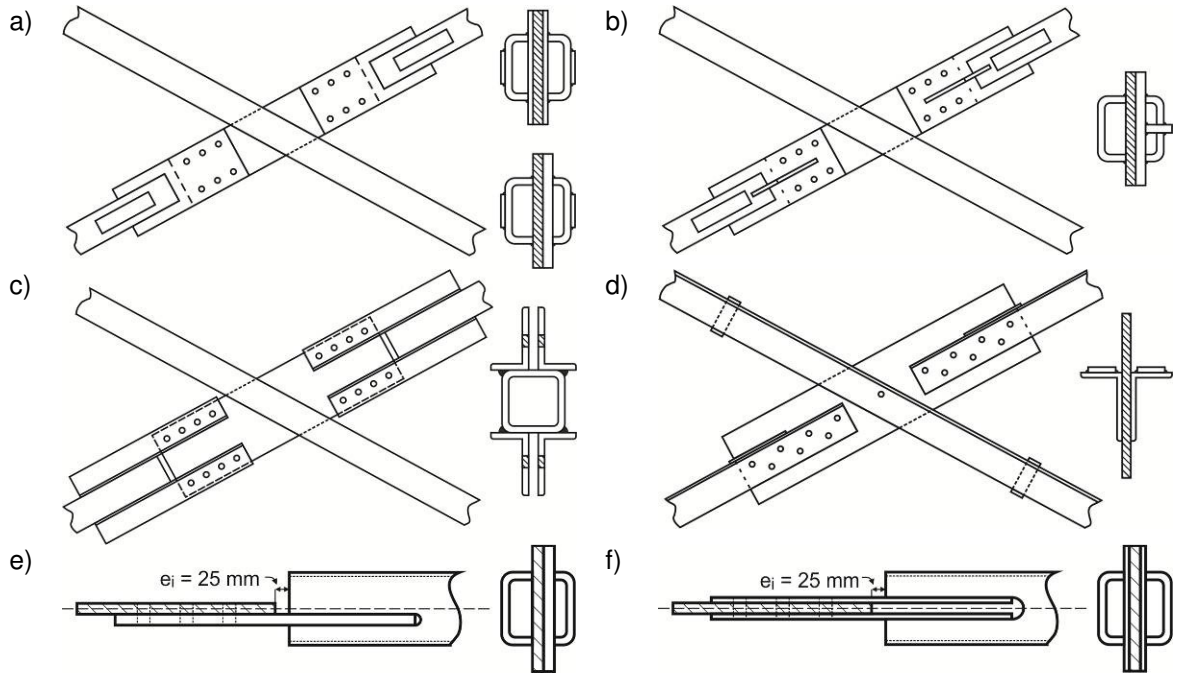

Figure 2 : Mid-connection details: a) SS and DS connections for HSS braces (Specimens nos. 5 to 14); b) Specimen no. 9; c) Specimen no. 4; d) Specimens nos. 16 to 18 with double angle brace; e) Top view of HSS SS connection; and f) Top view of HSS DS connection.

Table 1 : Characteristics of Test Specimen

No.	Braces	Type	Mid-Connection details			Design Loads			Test Results	
			b_g (mm)	t_g (mm)	n_b - d_b (mm)	T_{fc} (kN)	C_{fc} (kN)	C_r (kN)	$C_{ue,Dis}$ (kN)	$C_{ue,Con}$ (kN)
4	HSS127x127x8.0	MD-DS	305	19	8-22	1564	1061	686	1125	984
5	HSS127x127x8.0	CCS-DS	260	16	6-22	1029	1029	686	677	769
6	HSS127x127x8.0	CCS-DS	220	19	6-22	1029	1029	686	847	948
7	HSS127x127x8.0	CCS-SS	280	16	6-32	1029	1029	686	453	808
8	HSS127x127x8.0	CCS-SS	204	25	6-32	1029	1029	686	535	763
9	HSS127x127x8.0	CCS-SS	280	16	6-32	1029	1029	686	829	871
10	HSS127x127x8.0	CCM-DS	180	16	4-22	686	686	686	586	629
11	HSS127x127x8.0	CCM-DS	320	9.5	4-19	686	686	686	474	550
12	HSS102x102x6.4	MD-DS	240	16	6-22	998	516	348	477	604
13	HSS102x102x6.4	CCM-DS	152	16	4-16	348	348	348	433	474
14	HSS102x102x6.4	CCM-SS	152	16	4-22	348	348	348	284	483
16	2L127x76x9.5	CCM-DS	305	8.0	5-16	365	365	365	266	490
17	2L127x76x9.5	CCS-DS	254	9.5	5-19	559	559	372	313	507
18	2L127x76x9.5	MD-DS	305	16	7-22	1421	615	403	804	764

The connections were designed and detailed assuming braced frames of the Type MD (moderate ductility) and Type CC (conventional construction) categories, as defined in CSA S16-09. For the former, the connections were designed for the brace forces $T_{fc} = T_u$ in tension and $C_{fc} = C_u$ in compression, where T_u and C_u are the probable tensile and compressive resistances of the braces determined with the brace

probable yield strength, R_yF_y (= 460 MPa and 385 MPa for HSS and angle members, respectively). For Type CC frame specimens, the connections were designed for 1.5 C_r for the CCS type and 1.0 C_r for the CCM type, where C_r is the factored compressive resistance of the braces, assuming that the selected braces have a factored resistance C_r that exactly matches the brace design factored compressive design forces, C_f. The expected failure of CCS connections is non ductile and, as prescribed in CSA S16-09 for frames located in moderate and high seismic zones, connection design loads must be amplified by R_d = 1.5. That design load need not exceed the forces corresponding to the brace resistances T_u and C_u. The brace resistance C_r was determined using the brace nominal properties, the specified yield strength, F_y (= 345 MPa for HSS and 300 MPa for angles), and an effective length KL = 3331 mm. The latter was obtained assuming K = 0.5 and taking L as the clear brace length between gusset plates estimated at the design stage as equal to 0.78 times the beam-to-column center-to-center length. T_{fc} was always equal to or greater than C_{fc}, and all connection design were governed by tension resistance requirements. For SS connections, the eccentricity was neglected in design to obtain minimum connection sizes.

3 Observed Stability Response

3.1 Response of HSS X-Bracing with Single Shear (SS) Connections

All specimens with SS connections (nos. 7, 8, 9 and 14) exhibited similar behaviour. Nonlinear response was first observed when instability of the discontinuous brace acting in compression initiated at the mid-connection through bending of the middle plate in the free hinge distance e_i close to the HSS end. A plastic hinge eventually developed at that location and a three-hinge mechanism then formed in one of the discontinuous brace segment. The second and third hinges of that mechanism respectively developed in the middle plate, near the continuous brace, and in the splice plate connecting to the corner gusset plate, at the other end of the brace segment (Figure 3a). This buckling mode was different than buckling of the bracing member with plastic hinges forming in the middle of the HSS brace segment. As anticipated in design, buckling of the continuous braces occurred in the bracing members, within one half-segment of the braces (Figure 3b), confirming that the discontinuous braces acting in tension can provide out-of-plane lateral support to the continuous braces. However, observations of the specimens responses suggests that a three-hinge buckling mode could have also developed in the continuous braces, with one hinge in the mid-connection and two hinges in the splice and gusset plates at the frame corners. Probably, this behaviour did not occur because the test frame had been designed with corner gusset plates much thicker than necessary such that they could be re-used in all tests.

a) b)

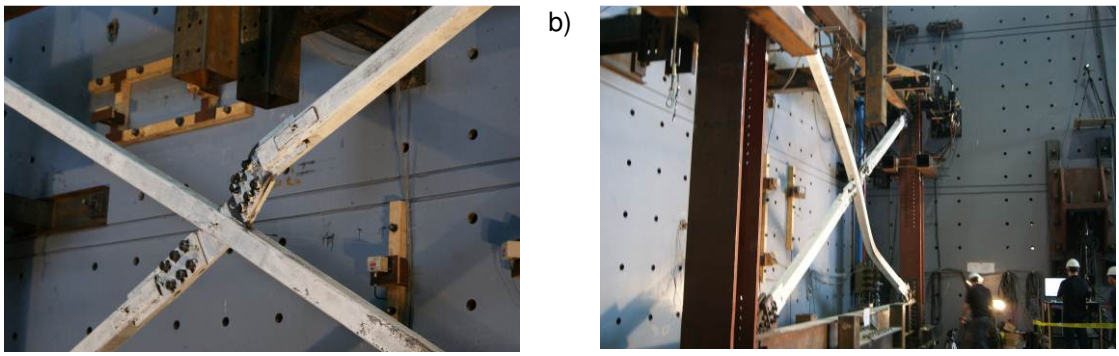

Figure 3 : Buckling response of HSS X-bracing with SS connections (Specimen no. 8):
a) Discontinuous brace; b) Continuous brace.

Specimens nos. 7 and 8 were identical except for the thickness of the middle plate. Using a thicker plates in Specimen no. 8 (25 mm *vs* 16 mm) resulted in a higher buckling load for the discontinuous brace ($C_{ue,Dis}$ = 535 kN *vs* 453 kN). A thicker plate also resulted in improved brace post-buckling behaviour and larger frame storey drift at failure. Specimen no. 9 was identical to Specimen no. 7 except that a stiffener had been added to the splice plates at the mid-connection. Although this modification resulted in a much higher compressive resistance for the discontinuous brace (829 kN *vs* 453 kN), this detail could not prevent the formation of the three-hinge mechanism as the stiffener was torn due to the high flexural

tension stresses that developed upon buckling. After failure of the stiffener, the brace compressive resistance rapidly degraded within a few loading cycles. Eventually, the compressive resistance was governed by the flexural strength of the middle plate acting alone and decreased to the resistance exhibited by the discontinuous brace of Specimen no. 7.

The hysteretic response of Specimen no. 8 is presented in Figure 4. In this and subsequent similar plots, the brace loads are normalized to the actual tensile resistance of the braces, T_{ua}, as calculated with the measured geometrical and mechanical properties. The corresponding actual compressive resistances, C_{ua}, were calculated with KL = 0.5 times the actual lengths of the continuous HSS braces (between 6492 and 6523 mm). In the plots, the loads T_{fc} and C_{fc} used for the design of the connections are also shown for reference and the frame lateral displacements are normalized with respect to the storey height, h_s (= 4087 mm). Significant differences can be seen between the discontinuous and continuous braces in compression. Compared to the continuous brace, buckling of the discontinuous brace occurred at a lower load and, consequently, at a lower storey drift. The three-hinge mechanism in the discontinuous brace also resulted in smaller post-buckling compressive resistance. That mechanism formed well below the brace connection design load C_{fc}. For the continuous brace, the buckling strength was close to C_{ua} predicted with the measured properties and buckling occurred at a load lower than the connection design load C_{fc}. The connections of both braces were able of carrying the connection design tension load T_{fc}.

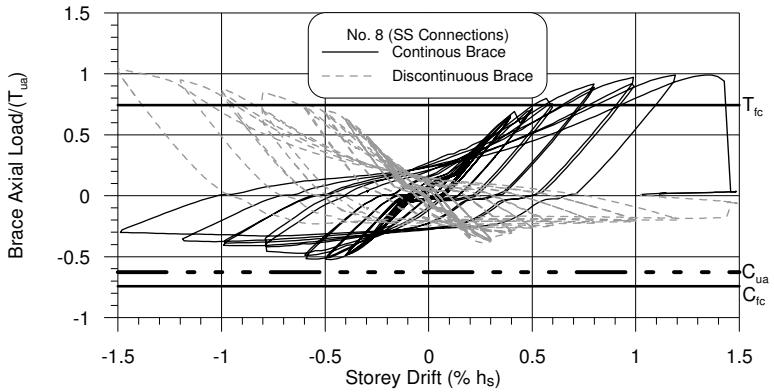

Figure 4 : Hysteresis of HSS X-bracing with SS connections (Specimen no. 8).

3.2 Response of HSS X-bracing with Double Shear (DS) Connections

The double shear connections were initially detailed without shim plates filling the gap between the splice plates inserted in the HSS members. Specimen no. 13 was tested with this connection detail. For both the discontinuous and continuous braces, buckling was triggered by flexural yielding of the splice plates in the free distance e_i next to the HSS end (Figure 2f), and a three-hinge plastic mechanism eventually formed as in the SS connection specimens. For the discontinuous brace, buckling initiated at the mid-connection (Figure 2a) and was limited to the lower brace segment. For the continuous brace, instability initiated in the lower corner connection (Figure 2b) and the three-hinge mechanism involved the full brace length with the third hinge forming in the opposite corner connection. Under larger storey drifts, inelastic rotation also developed in the two HSS halves at the end of the slot created to insert the splice plates (Figures 5a and 5b). In that fourth hinge, yielding took place in the two HSS halves and cracking eventually appeared in the HSS, near the splice plates, when the bent HSS halves were straightened up upon reloading the brace in tension (Figure 5c). Cracks were promoted by non uniform tensile strains in the HSS resulting from shear lag effects in the HSS and unequal tension forces between the two splice plates due to previous deformations experienced upon buckling. Opening of the HSS at the slot was also observed due to lack of attachments between the two splice plates. Tearing of the welds connecting the splice plates to the HSS was also noticed. During the test, energy dissipation in Specimen no. 13 was concentrated in plate and HSS local deformations taking place in the connections. Residual deformations of the splice plates after several cycles of stretching in tension and buckling in compression are shown in Figure 5d. In view of this poor behaviour, shim plates were used in all other DS specimens. In Specimens nos. 10 and 12, the shim plates were only tack welded to the splice plates. As shown in Figure 6 for Specimen no. 12, the behaviour of both specimens was nearly identical to that of Specimen no. 13, plus subsequent

inelastic bending in the HSS at the end of the slots, forming in the continuous and discontinuous braces. Tack welds broke in most buckled connections and some fell off the connections. Opening of the HSS section was also observed.

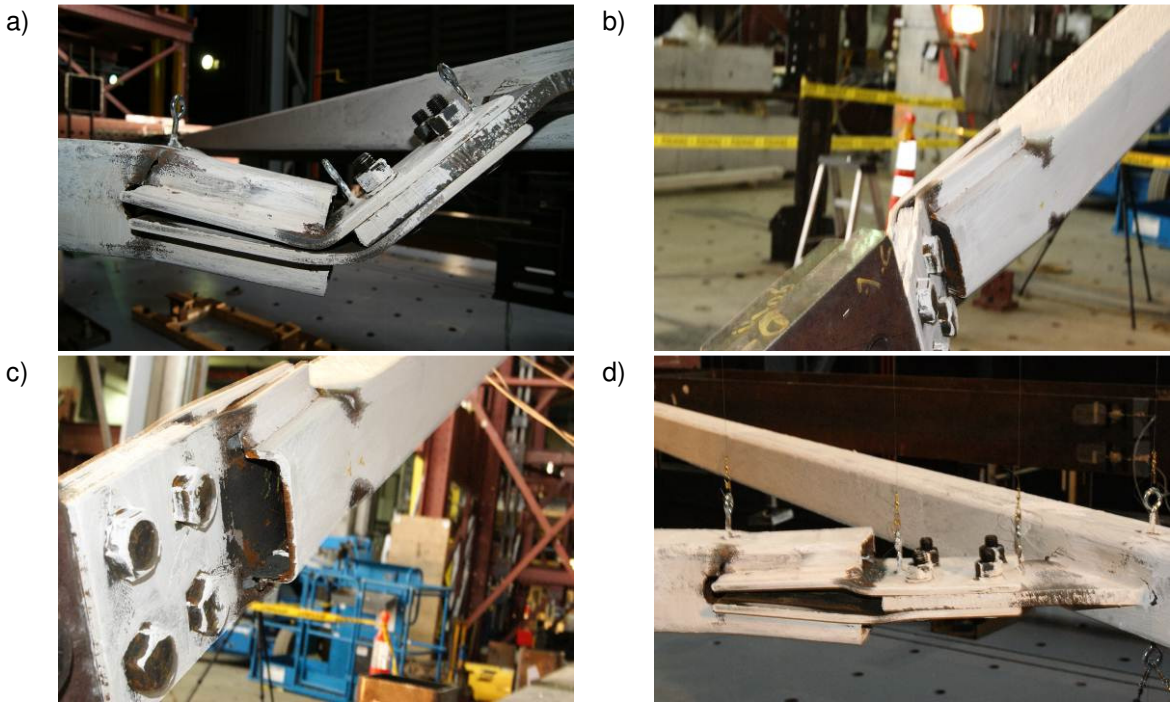

Figure 5 : Damage to connections after buckling in HSS X-bracing with DS connections without shim plates (Specimen no.13).

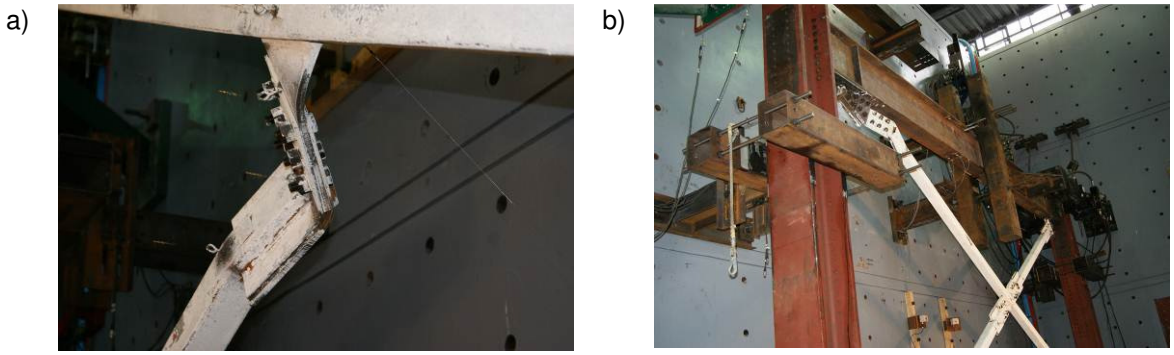

Figure 6 : Connection buckling in Specimen no. 12 with DS connections and tack welded shim plates: a) At mid-connection; b) At gusset plate connection.

For Specimens nos. 5, 6 and 11, the shim plates were connected using continuous structural welds. In all three specimens, buckling of the discontinuous brace was similar to that observed in the previous DS specimens except that for Specimen no. 11, two hinges formed in the corner gusset plate, in the free distance e_i and in the gusset plate, whereas the third hinge formed in the middle plate of the mid-connection. For the continuous brace, the same two hinges formed in one corner connection and the third hinge developed in the opposite corner connection. Structural continuous welding of the shim plates mitigated individual response of the HSS half-sections on either side of the end slots and the inelastic rotations in the HSS at the slot ends were therefore reduced compared to previous HSS specimens with DS connections. No or very limited cracking developed in the HSS of these specimens as shown in Figure 7a. For Specimen no. 6, rupture of the shim plate welds occurred at the mid-connection. This failure did not influence much the post-buckling resistance of the specimen because failure of the specimen occurred at another location a few cycles later.

a) b)

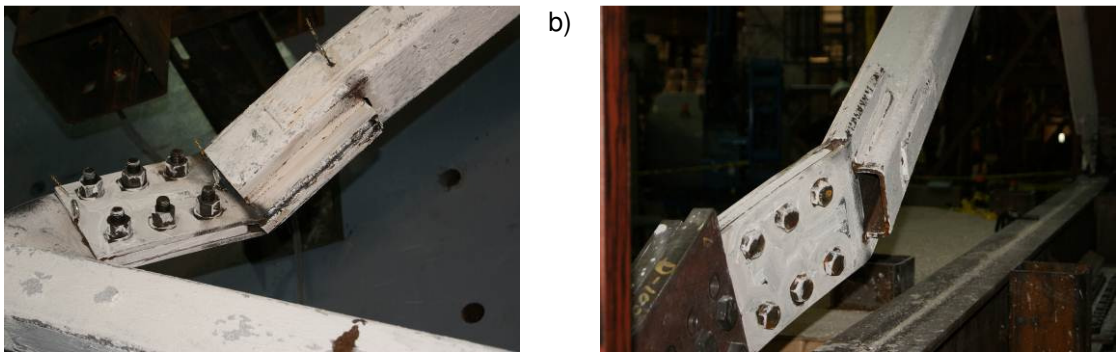

Figure 7 : Mechanism in DS connections with continuously welded shim plates (Specimen no. 6): a) At mid-connection; b) At gusset plate connection.

In addition to limiting localized inelastic deformations and damage in the connections, the use of shim plates with continuous structural welds resulted in higher brace compressive resistances, enhanced post-buckling brace behaviour and more stable response in tension due to reduced HSS cracking. This is illustrated in Figure 8 where the hysteresis of one specimen with tack welded shim plates (Specimen no. 12) is compared to that of Specimen no. 6 with continuously welded shim plates. For Specimen no. 12, the loss of compressive strength due to connection buckling is more pronounced than for Specimen no. 6. In addition, in Specimen no. 12, several occurrences of fracture of the discontinuous HSS section are evidenced by the successive resistance drops in tension. This behaviour was not observed in Specimen no. 6. For both specimens, all connections reached their design load T_{fc}. Among all HSS specimens with DS connections, these two frames exhibited the highest brace compressive resistances relative to C_{ua} and the only two specimens for which the continuous brace exceeded C_{ua} in compression. For the other specimens, the compressive resistance of the continuous brace was less than C_{ua}.

a) b)

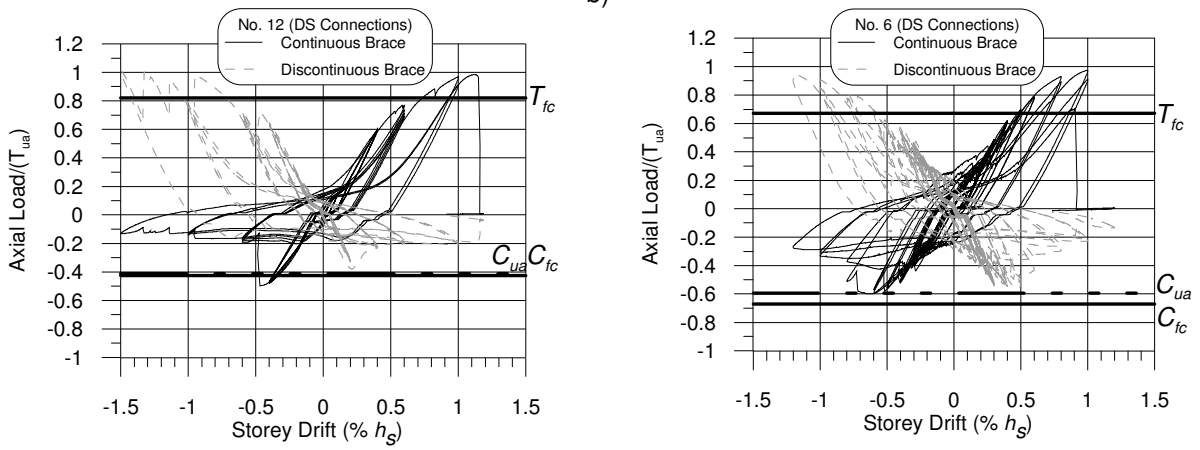

Figure 8 : Hysteresis of HSS X-bracing with DS connections and: a) Tack welded shim plates; b) Continuously welded shim plates.

The connections of Specimen no. 4 were designed with angles connecting the HSS members to the middle or gusset plates (Figure 2c). As done in practice, four angles were used for each connection, on either side of the HSS and of the splice plates, to obtain concentric connections. The angles provided relatively higher flexural stiffness and strength to the connections and this specimen is the only one where buckling of the two braces took place in the bracing members. Local buckling of the HSS walls was observed at large storey drifts, as expected for HSS bracing members (Tremblay et al. 2003).

3.3 Response of Double Angle X-bracing

As shown in Figure 9a, buckling of the discontinuous brace in Specimens nos. 16 and 17 occurred in the mid-connection of the discontinuous braces, as was observed after the Tōhuku earthquake (Figure 1b). This instability induced significant out-of-plane bending of the middle plate. Contrary to HSS braces, buckling also involved pronounced torsional deformations of the continuous brace. The difference is attributed to the fact that double angle sections exhibit much lower torsional stiffness compared to HSS members. Specimen no. 18 was designed with a thicker middle plate (16 mm *vs* 8.0 and 9.5 mm) and buckling of the discontinuous brace took place over half of the brace length, as intended in design. For all three double angle specimens, buckling of the continuous brace occurred in the brace itself (Figure 9b) and at a load exceeding C_{ua}. The hysteretic response of Specimen no. 16 is presented in Figure 10a. For this specimen, the connections of both braces were able to resist the design tension loads T_{fc}. Due to local instability at mid-connection, the compressive resistance of the discontinuous brace did not reach C_{ua} and was much lower than that of the continuous brace. CCM connections detailed to exhibit ductile behaviour through bearing of the bolts were used in that specimen. As shown in Figure 10, the connections could develop the design force T_{fc} and exhibit the intended ductile response.

a) b)

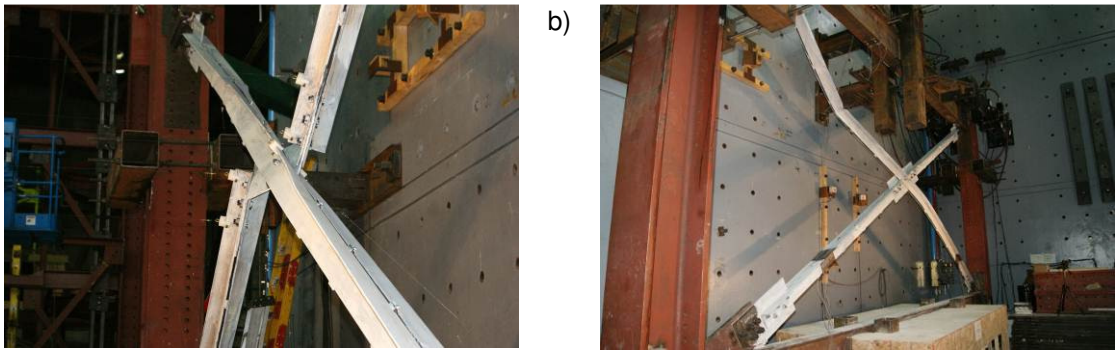

Figure 9 : Buckling in 2L X-bracing (Specimen no. 16): a) Buckling at mid-connection for the discontinuous brace; b) Buckling of the continuous brace.

a)

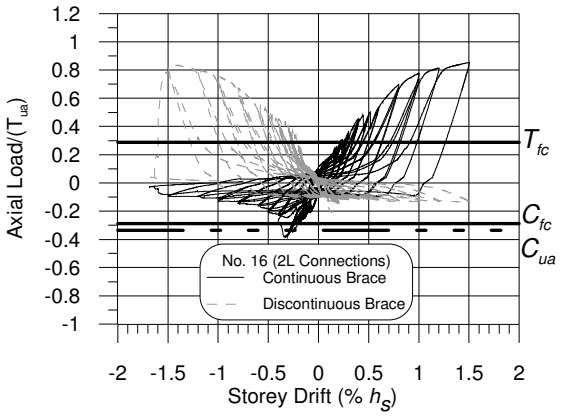

b)

Figure 10 : 2L X-bracing (Specimen no. 16): a) Hysteresis; b) Bearing at bolt holes.

3.4 Observed Failure Modes

The observed failure modes are presented in Figure 11. Except for Specimen no. 18, failure of all specimens took place in the brace connections when subjected to tension loading. For Specimen no. 18, failure occurred in the bracing members under tension, after local buckling has occurred. For HSS Specimens nos. 5, 7, 9 and 14, failure took place in the splice plates at mid-connection, in the free distance e_i at the end of the discontinuous brace (Figure 11a). This rupture is attributed to low-cycle fatigue in bending together with stress concentrations due to shear lag caused by the welds connecting the splice plates to the HSS. For Specimen no. 6, rupture at net section of the bolted connection was observed at the end of the continuous brace (Figure 11b). Rupture of Specimens nos. 4 and 8 occurred in

tension at the reduced net section in the continuous brace created by the slots for the middle plate (Figure 11c). Evidence of shear lag effects due to the load transfer from the continuous brace to the middle plate could be observed, indicating that shear lag effects should therefore considered at this location in design calculations. For Specimens nos. 12 and 13, tension failure occurred at the HSS net section at the end of the slots (Figure 11d). For Specimen no. 11, failure took place in the corner gusset plate (Figure 11e). This failure is attributed to low-cycle fatigue due to low-cycle fatigue in bending induced by the three-hinge mechanism. In Specimens nos. 10, 16 and 17, the rupture was observed in the middle plate (Figure 11f). Net section failures shown in Figures 11a to 11d occurred in 12 out of the 17 specimens of the test program. Rupture of a test specimen was said to have occurred when the storey shear reduced to 80% of the peak storey shear value. For Type CC braced frame specimens, the rupture was observed at storey drifts varying from 0.4% to 1.5% h_s, with an average value of 1.0% h_s. For Type MD frames, storey drifts at rupture ranged between 1.1% and 1.7% h_s, with an average value of 1.4% h_s.

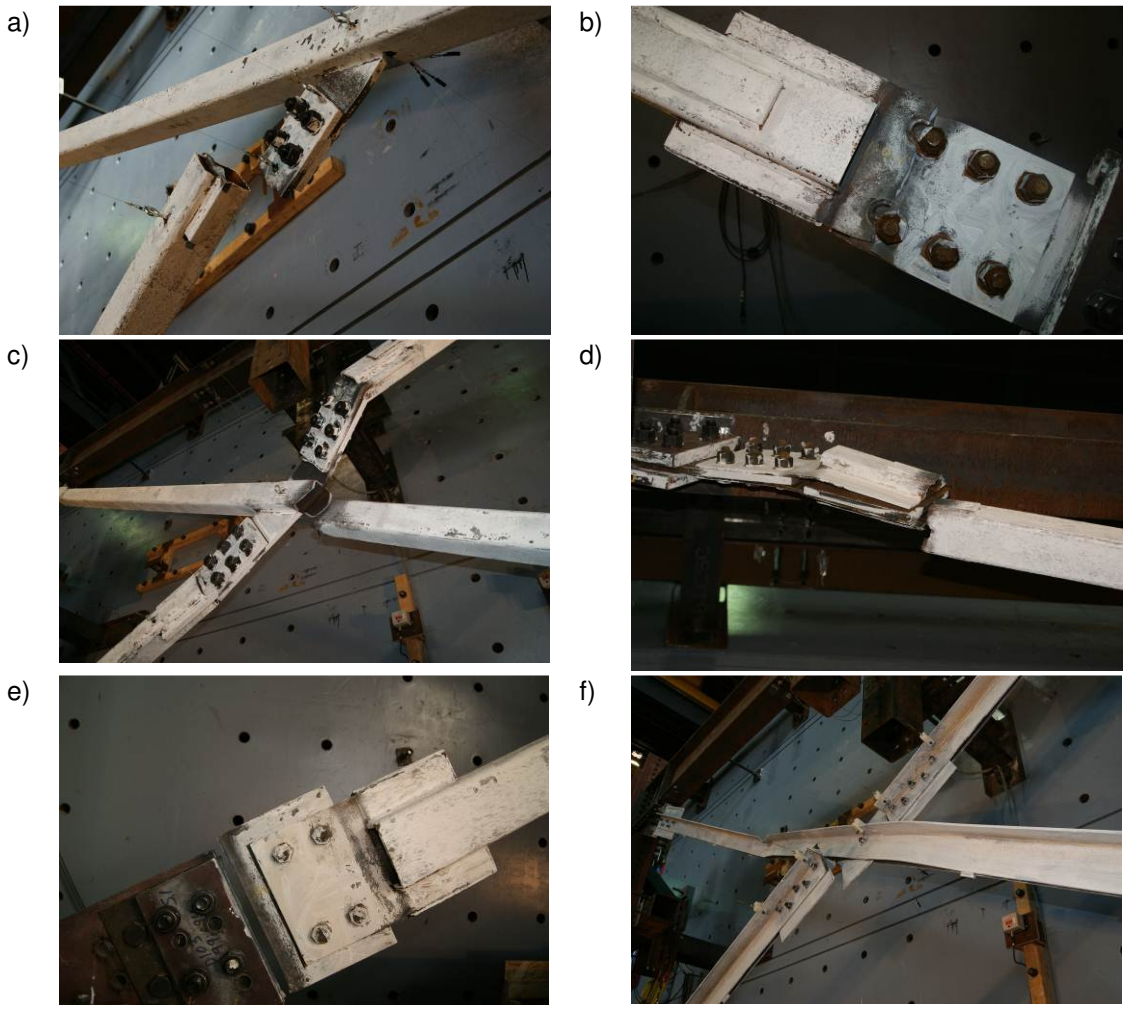

Figure 11 : Observed failure: a) at net section in middle plate; b) at net section in splice plates; c) at net section of continuous brace at middle plate; d) at net HSS section; e) in gusset plate; f) in middle plate.

4 Conclusions and Recommendations

A quasi-static cyclic experimental program was performed on steel X-braced frames to investigate the stability response of the bracing members including the effects of local deformations occurring in the connections. HSS and double angle bracing members assembled with typical bolted connections were studied and connection designs complied with CSA S16 requirements for Type MD and Type CC braced frames. The main conclusions of this study can be summarized as follows:

- In specimens with single shear and double shear splice plate connections, buckling of the discontinuous brace member was triggered by local bending of the connection plates. Buckling was followed by a plastic mechanism formed with hinges developing in the connection plates only, not in the bracing members. The measured compressive resistance of these specimens was less than the brace predicted actual compressive resistance. The tests showed that this response can be mitigated by increasing the flexural stiffness and strength of the connections.
- In all specimens, the discontinuous brace provided out-of-plane lateral support to the continuous brace. For the HSS specimens with splice plate connections, however, the compressive resistance of the continuous brace was generally less than that predicted by calculations. For the double angle braces, the continuous brace could reach its predicted capacity.
- When a plastic mechanism formed with hinges located in the connection plates, energy essentially dissipated through inelastic rotations in connection plates rather than in the bracing members, which resulted in reduced brace compressive resistance and energy dissipation capacity in the post-buckling range.
- Double shear splice connections with continuously welded shim plates exhibited superior inelastic cyclic performance compared to connections without shim plates or with tack welded shim plates.
- Except for one specimen, failure took place in connections under tension loading. Inelastic rotation that developed in the connection components reduced the ductility and strength of the connections, even in Type MD specimens.
- Shear lag effects must be considered at the net section of the continuous brace resulting from the slot created for inserting the middle plate.
- Future work should include the development of equations for the prediction of the compressive resistance of braces including connection flexibility effects.

Acknowledgements

Financial support for this project was provided by the Natural Sciences and Engineering Research Council of Canada. The contribution of Atlas Tube, Beauce-Atlas and the Canam Group for the fabrication of the test specimens is acknowledged. The authors thank Mr. Carl Boutin and Daniel Mongeau of SDK, Montreal, Qc, and Eric Dumont of Beauce-Atlas, Ste-Marie, Qc, for their most valuable technical input and advices. They also acknowledge the assistance of the technical staff of the Structural Engineering Laboratory at Ecole Polytechnique in the test program.

References

Astaneh-Asl, A., Goel, S.C., and Hanson, R.D. 1985. Cyclic out-of-plane buckling of double angle bracing. *Journal of Structural Engineering*, ASCE, 111(5): 1135-1153.

CSA. 2009. *CSA-S16-09, Design of Steel Structures*, Canadian Standards Association, Mississauga, ON.

Davaran, A. 2001. Effective length factor for discontinuous X-bracing systems. *Journal of Engineering Mechanics*, ASCE, 127(2): 106-112.

Davaran, A., and Hoveidae, N. 2009. Effect of mid-connection detail on the behavior of X-bracing systems. *Journal of Constructional Steel Research*, 65(4): 985-990.

Gélinas, A., Tremblay, R., and Davaran, A. 2012. Seismic Behavior of Steel HSS X-Bracing of the Conventional Construction Category. *Proc. Structures Congress 2012*, ASCE, Chicago, IL: 1649-1660.

EERI. 2011. Effects of the 2011 Tohoku Japan Earthquake on Steel Structures. EERI Steel Structures Reconnaissance Group. Consulted on 2013 January 1st, from : http://www.eqclearinghouse.org/2011-03-11-sendai/2011/08/03/eeri-steel-structures-reconnaissance-group/

Picard, A., and Beaulieu, D. 1988. Design of diagonal cross-bracings. Part 2: Experimental study. *Engineering Journal*, AISC, 25(4): 156-160.

Segal, F., Levy, R., and Rutenberg, A. 1994. Design of imperfect cross-bracings. *Journal of Engineering Mechanics*, ASCE, 120(5): 1057-1075.

Tremblay, R., Archambault, M.H., and Filiatrault, A. 2003. Seismic Performance of Concentrically Braced Steel Frames made with Rectangular Hollow Bracing Members. *Journal of Structural Engineering*, ASCE, 129(12): 1626-1636.